Direct Cell Lineage Analysis in *Drosophila melanogaster* by Time-Lapse, Three-Dimensional Optical Microscopy of Living Embryos

Jonathan S. Minden, David A. Agard,* John W. Sedat,* and Bruce M. Alberts

Department of Biochemistry and Biophysics, and *Howard Hughes Medical Institute Structural Biology Unit, University of California, San Francisco, San Francisco, California 94143

Abstract. One of the first signs of cell differentiation in the *Drosophila melanogaster* embryo occurs 3 h after fertilization, when discrete groups of cells enter their fourteenth mitosis in a spatially and temporally patterned manner creating mitotic domains (Foe, V. E., and G. M. Odell. 1989. *Am. Zool.* 29:617–652). To determine whether cell residency in a mitotic domain is determined solely by cell position in this early embryo, or whether cell lineage also has a role, we have developed a technique for directly analyzing the behavior of nuclei in living embryos. By microinjecting fluorescently labeled histones into the syncytial embryo, the movements and divisions of each nucleus were recorded without perturbing development by using a microscope equipped with a high resolution, charge-coupled device. Two types of developmental maps were generated from three-dimensional time-lapse recordings: one traced the lineage history of each nucleus from nuclear cycle 11 through nuclear cycle 14 in a small region of the embryo; the other recorded nuclear fate according to the timing and pattern of the 14th nuclear division. By comparing these lineage and fate maps for two embryos, we conclude that, at least for the examined area, the pattern of mitotic domain formation in *Drosophila* is determined by the position of each cell, with no effect of cell lineage.

OBSERVATIONS made with the light and electron microscope have produced a detailed description of the morphological changes that occur throughout the early development of the *Drosophila melanogaster* embryo (Rabinowitz, 1941; Sonnenblick, 1950; Turner and Mahowald, 1976; Zalokar and Erk, 1976; Foe and Alberts, 1983). Once fertilized, the zygotic nucleus in this giant oval-shaped cell undergoes 13 cycles of nearly synchronous mitotic division, creating a syncytium. Throughout the first six mitotic cycles the nuclei reside in the interior of the embryo, but they begin to migrate toward the surface of the embryo during the seventh nuclear cycle. A few nuclei reach the posterior end of the embryo in their ninth nuclear cycle and become cellularized, creating the "pole cells" (germ cell progenitors). Most of the remaining nuclei reach the periphery of the embryo in the next nuclear cycle, forming an evenly spaced monolayer at the embryo surface. These "syncytial blastoderm" nuclei undergo four additional rounds of mitosis as a monolayer and then begin to cellularize 30 min after their 13th mitosis.

The transition from syncytial to cellular blastoderm is a pivotal point in the development of the embryo. As soon as cellularization is complete, the complex and rapid movements of gastrulation begin. Several rounds of mitosis occur during gastrulation (defined as the period beginning with ventral and cephalic furrow formation and ending with maximum germ band extension), and the numerous cell divisions have been analyzed by Hartenstein and Campos-Ortega (1985) and in more detail by Foe (1989). Instead of the synchronous nuclear divisions of the syncytial blastoderm, groups of cells divide at different times and in different orientations according to a precise and reproducible schedule. Foe (1989) has shown that these so-called mitotic domains are regularly oriented with respect to the 14 stripes of expression of the engrailed gene product, and has argued that each domain marks a region with a different cell fate. The pattern of mitosis thereby may serve as a very early indicator of the region-specific cell differentiation events that will form the larva.

Are the cells that reside in a particular mitotic domain clonally derived or are they selected solely as a function of their position in the embryo? Earlier studies of mosaic embryos suggest that determination occurs after cellularization in cycle 14 (Illmensee, 1976; Simcox and Sang, 1983; Garcia-Bellido and Merriam, 1969; Janning, 1978). To examine this question on a cell-by-cell basis, we have developed a technique for marking nuclei at the syncytial blastoderm stage and continuously following their behavior through many divisions. Nuclei in the early embryo can be clearly visualized by microinjecting fluorescently labeled histone proteins that become incorporated into the chromatin of replicating DNA. A map of the divisions of these nuclei was generated by continuously examining the progeny of >40 nuclei in a small area of the embryo from nuclear cycle 11 to the end of cycle 14 with a scientific grade, charge-coupled device (CCD)[1] mounted on an inverted fluorescence micro-

1. *Abbreviations used in this paper*: CCD, charge-coupled device; NHSR, *N*-hydroxy-succinimide tetramethyl rhodamine.

scope. Because the two-dimensional monolayer of nuclei becomes highly distorted once gastrulation begins, a complete tracing of nuclear divisions required three-dimensional, time-lapse movies; these were generated by recording images taken at regularly spaced focal planes in a cyclical fashion and then computationally manipulating each focal series to generate a pair of stereo images (Agard, 1984; Hiraoka et al., 1987; Agard et al., 1988).

From these data, we determined that cells of the same lineage can reside in different mitotic domains, that partitioning of related cells across domain boundaries is apparently random, and that the cell lineage pattern is not repeated between two embryos. We conclude that cell fate is probably specified by positional cues without regard to lineage history.

Materials and Methods

Preparation of Fluorescently Labeled Histone Proteins

A detailed protocol for labeling histone proteins will be published elsewhere (Minden, J., manuscript in preparation). Briefly, purified histones were bound to double stranded DNA cellulose under conditions that permit nucleosome formation (Palter and Alberts, 1979). The purpose of this step was to ensure that only the exposed surface of the proteins were modified during a 30-min room temperature incubation with *N*-hydroxy-succinimide tetramethyl rhodamine (NHSR) (Molecular Probes Inc., Junction City, OR) in a buffer containing 0.2 M NaCl, 20 mM potassium Hepes, pH 7.4, and 1 mM Na_3EDTA. After the unreacted fluorochrome was removed by repeated washing of the resin, the NHSR-labeled nucleosome/DNA cellulose resin was packed into a small column and the histone proteins were eluted with a 0.2–2.0-M NaCl gradient containing 20 mM Tris-HCl, pH 7.4, and 1 mM Na_3EDTA. The fractions that contained histones H2A and H2B, determined by PAGE, were pooled and concentrated by centrifugation in a spin dialysis apparatus (Centricon 10; Amicon, Danvers, MA). Small aliquots were frozen in liquid nitrogen and stored at −80°C. The stored NHSR-histones prepared and stored in this fashion were stable for more than 1 yr.

Microinjection of the NHSR-Histones

Wild-type Oregon R embryos were collected at 10-min intervals on small Petri dishes that contain standard egg laying media (Roberts, 1986). The embryos were hand dechorionated and mounted on a 20 × 50-mm coverslip through the use of a thin strip of glue prepared by dissolving the adhesive from double-sided Scotch-brand tape in heptane. The embryos were dried slightly over $CaCl_2$ for 8–12 min and then overlayed with a drop of halocarbon oil (series 700; Halocarbon Products, Hackensack, NJ). Injections of a 0.4-mg/ml solution of NHSR-histone H2A/2B protein were made at 50% egg length using a Lietz micromanipulator. Injection needles (3 μm diam) were pulled from 1.2 mm OD × 0.9 mm ID glass capillary tubes (omega dot type; FHC, Brunswick, ME). The time from collection to injection was <30 min, so that the labeled protein could diffuse evenly throughout the embryo cytoplasm before cycle 10 and produce uniformly labeled blastoderm nuclei.

Recording the Movements of the Chromatin Labeled with NHSR-Histone

The NHSR-histone-injected embryos were observed on an Olympus inverted microscope equipped for epifluorescence, using a 40×, 1.3 NA, oil immersion objective lens (Olympus) and a high performance rhodamine filter set (Omega Optical Inc., Brattleboro, VT). The embryo was illuminated with a 100-W mercury arc lamp attenuated 20-fold with a 520 ± 10-nm band pass filter (Omega Optical Inc.). The images were acquired by a Peltier-cooled CCD camera (Photometrics Ltd., Tucson, AR) equipped with a 1,340 × 1,037 pixel CCD chip (Kodak-Videk). The entire process of focusing the objective, opening and closing shutters, and storing the digital data was controlled by a Microvax II workstation (Digital Equipment Corp. Marlboro, MA) coupled to a 32 M-byte Mercury Zip 3232+ array processor (Mercury Computer systems Inc., Lowell, MA) and a display system (model 1280; Parallax Graphics Inc., Santa Clara, CA). The data was stored on a large format, 2 G-byte, optical disk (Emulex Corp./Optimem 1000, Costa Mesa, CA). A typical recording was made in two parts; the first segment captured the syncytial divisions as a series of single focal plane exposures of 0.1 s taken every 23 s, while the second segment began at cellular blastoderm and recorded the cycle 14 mitoses as a repeating series of similar exposures taken at eight consecutive focal planes spaced 2.5 μm apart (the focal series was repeated every 23 s). Only the top six focal planes were used to generate the three-dimensional movies, because the two deepest sections contained unincorporated or degraded NHSR-histone that blurred the images. The embryos were kept until hatching to ensure that neither the injection of histones nor the illumination during the recording session had damaged the embryo.

Data Manipulation and Computer Programming

The bulk of the data processing and computer model building were performed on a Vax 8650 computer system (Digital Equipment Corp.) with attached Parallax display stations. All of the software used is also compatible with the Microvax II system. To obtain high quality stereo projections of the three-dimensional data stacks, the images were computationally manipulated to enhance the local contrast around each pixel (Belmont et al., 1987). Each set of optical sections was then converted into a three-dimensional array of pixel intensities, rotated in space, and projected onto an imaginary image plane to produce a pair of stereo images (Agard et al., 1988).

The tracings shown were generated interactively with the computer graphics display system, by entering selected data with an on-screen cursor. The modeling software package, written in Fortran, allows the viewing of simultaneously updated stereo images in a time-lapse fashion (Chen, H., and D. A. Agard, manuscript in preparation). The images shown here were photographed using a Dunn digital camera system (Log E-Dunn) with Technical Pan 2415 film.

Results

Tracing Nuclear Behavior from Cycle 11 to the Completion of Cycle 14

The 5,000 cells that form the cellular blastoderm in cycle 14 can be subdivided into at least 25 mitotic domains that seem to reflect the result of spatially patterned cell determination processes (Foe, 1989; Foe and Odell, 1989). To test for a possible role of cell lineage in these cell determination events, we have followed the detailed behavior of the nuclei in an area of the embryo that contains several intersecting mitotic domains. The field of view is shown as an unshaded area in Fig. 1; it encompasses a lateral region anterior to the cephalic furrow that will form six mitotic domains. This region contains >40 nuclei at nuclear cycle 11; in 3 h, at 23°C, it developed from nuclear cycle 11 through the end of cycle 14 (four nuclear divisions), producing >300 cells that can be grouped into mitotic domains according to the time and pattern of the cell division that ends their 14th nuclear cycle. Most of the data presented here were generated from a single embryo that went on to generate a normal larva after the recording was terminated.

Fluorescent Marking of the Nuclei

Syncytial nuclei were visualized by microinjecting fluorescently labeled calf-thymus histones, which became incorporated into chromatin during subsequent periods of DNA replication. To ensure that the fluorescent histones were distributed evenly throughout the syncytial cytoplasm, injections were performed within 30 min of egg deposition (before nuclear cycle 5). Our previous studies demonstrated that these calf-thymus histones do not interfere with normal development in unirradiated embryos (Minden, J. S., and B. M. Alberts, manuscript in preparation). Although prolonged ir-

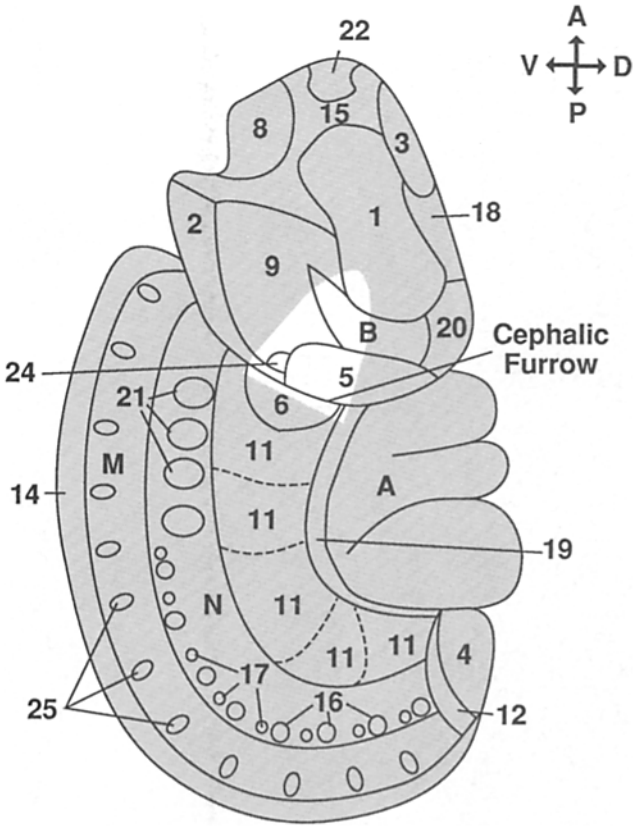

Figure 1. Lateral view of cycle 14 mitotic domains. Detailed map of cycle 14 mitotic domains from Foe and Odell (1989). Unless stated otherwise, the embryo is oriented with the anterior end up and the ventral side on the left in all figures. The mitotic domains are assigned numbers to indicate the temporal sequence of domain mitoses, with letters to indicate groups of cells that either do not divide (*A* and *B*) or divide asynchronously (*M* and *N*). The unshaded area designates the field of view used in this work. Because we have focused on the domains anterior to the cephalic furrow, domain 6 was omitted from further analysis.

radiation of fluorescent histone-injected embryos with intense light is lethal, by exposing the embryo to brief pulses of attenuated light we can observe these nuclei for many hours without detectable damage to the embryo.

Following the Descendents of Single Nuclei from Cycle 11 to Cellular Blastoderm

A series of images of a living embryo taken at 0.375-min intervals that allow individual cycle 11 nuclei and their progeny to be traced through three syncytial divisions is presented in Fig. 2. The progeny of a single nucleus are marked to demonstrate the type of nuclear movements seen in the embryo. Each of the three vertical columns starts at metaphase of a nuclear cycle (cycles 11, 12, or 13, respectively) and continues through interphase and prophase of the following nuclear cycle. (A cycle is defined as beginning at interphase and ending at telophase.) Since the syncytial nuclei remain in the cortex of the embryo throughout this period, recordings can be made with a fixed focal plane. This sequence of live images demonstrates that the duration of anaphase plus telophase (two phases of mitosis that are not easily distinguished by chromosome staining alone) is 2.7 ± 0.4 min in all three nuclear cycles. The duration of prophase plus metaphase is also constant at 2.0 ± 0.2 and 2.5 ± 0.8 min, respectively. However, the length of interphase increases, being 5, 8, and 18 min, for cycles 11, 12, and 13, respectively. These observations agree with previous data obtained in other ways (Foe and Alberts, 1983).

Analysis of Nuclear Behavior before Gastrulation Using Computer Based Tools

After marking the location of the nucleus in every frame with an interactive cursor, a computer software package for two- or three-dimensional image analysis (Chen, H., and D. A. Agard, manuscript in preparation) was used to digitize, store, and organize all of the nuclear positions. Fig. 3 presents a display of the movements and divisions of the marked nuclei in Fig. 2. Because of the complexity of the movements, the data is presented as a stereo pair, in which the elapsed time is translated into depth. Each nuclear cycle displays a characteristic pattern of nuclear movement. Anaphase is characterized by a rapid separation of the daughter nuclei (straight lines in a single plane that diverge from the filled circle). The amount of movement of the nuclei during interphase increases from cycle 12 to cycle 14. In early interphase of cycle 14, the nuclei undergo a dramatic swirling motion (Fig. 3 *C*); subsequently, cellularization occurs by the inward furrowing of the egg plasma membrane, and the nuclei stay nearly fixed in position for 30 min (see Fig. 6, *B* and *C* below).

Except for the anaphase movements, all movements of neighboring nuclei are coordinated; so that the monolayer of nuclei tends to move as a unit. However, whereas the nuclei maintain an evenly spaced configuration during cycles 11 and 12, the nuclei in nuclear cycle 13 come very close to each other at the end of anaphase and form small, short-lived clusters of three to five nuclei (see Fig. 2 *C*, t = 1.50 min).

Lineage Map for a Patch of 40 Cycle 11 Nuclei

To produce a lineage map of the entire field of view shown in Fig. 1, the type of analysis presented in Fig. 3 for a single cycle 11 nucleus and its progeny was extended to include all of the nuclei in the field. Fig. 4 *A* shows the initial positions of the nuclei at the end of interphase of nuclear cycle 11. Fig. 4, *B* and *C* displays the positions of daughter nuclei at the end of interphase of nuclear cycles 12 and 13, respectively, while Fig. 4 *D* shows nuclear positions 30 min into interphase of cycle 14. Clusters of eight nuclei in Fig. 4 *D* that share the same marking are related by the previous divisions. Single nuclei were never found to be isolated from their siblings by being completely surrounded by unrelated nuclei; this clustering means that there is no nuclear mixing between nuclear cycle 11 and 14; the nuclei do not change their neighbors during this period. There is no obvious pattern in the direction of the mitoses within the plane of the syncytial monolayer or in the spatial arrangement of related nuclei as evidenced by the orientation of the line connecting daughter nuclei in Fig. 4. Every aspect of the mitoses that occur in the syncytial blastoderm stage embryo appears to be disordered.

Assigning Each of the Cycle 14 Cells to Their Respective Mitotic Domains

The field of view examined in Fig. 4 covers portions of seven

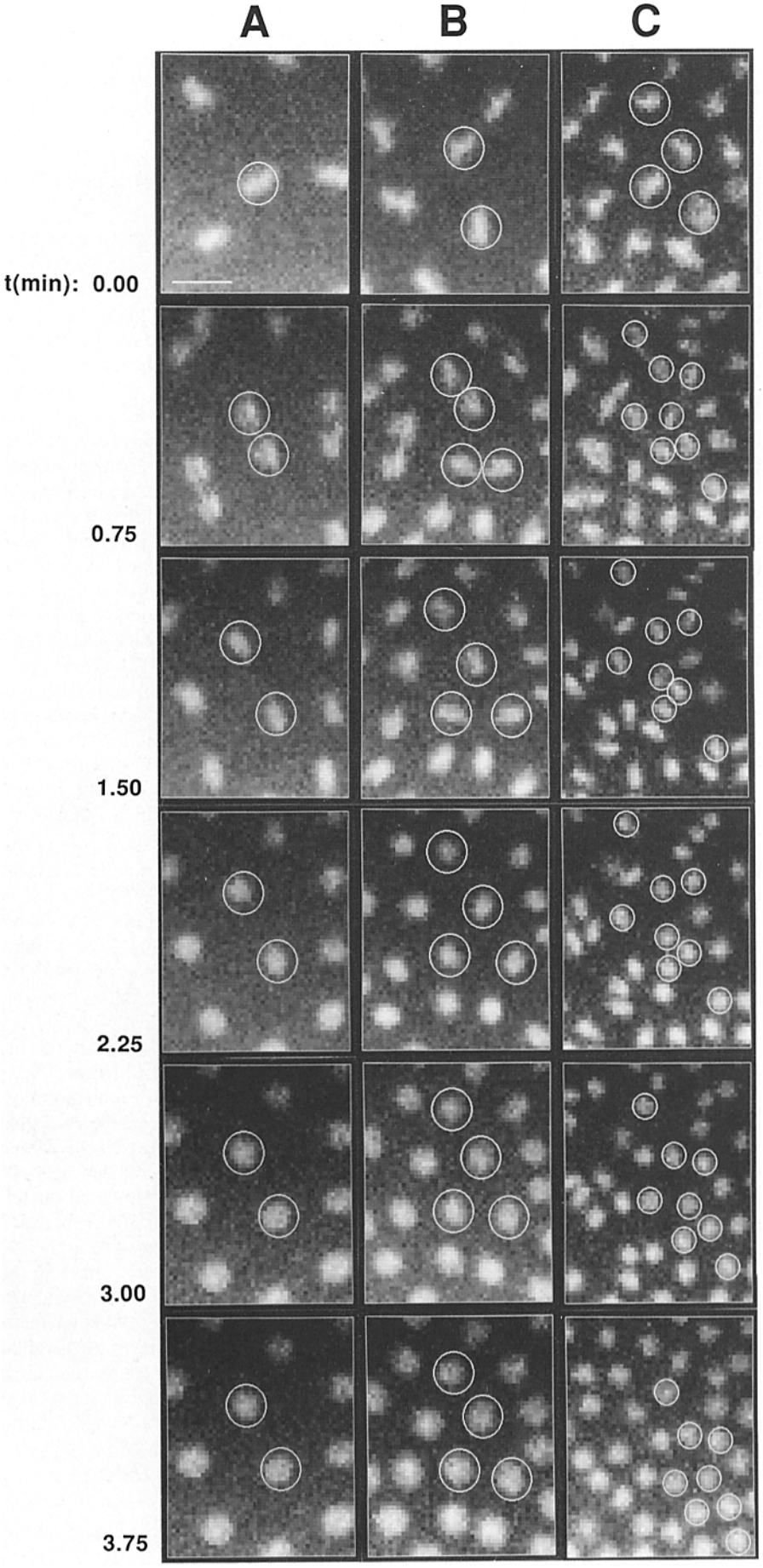

Figure 2. Fluorescent images of nuclei from metaphase of nuclear cycle 11 to interphase of nuclear cycle 14. A wild-type Oregon R embryo was hand dechorionated, mounted on its side on a coverslip, desiccated, and covered with halocarbon oil to prevent further drying. The embryo was then injected at 50% egg length with a 0.4 mg/ml solution of fluorescent histone H2A/H2B. The images were recorded as described in Results. A series of images of a small area of the field of view taken at the indicated intervals is shown to demonstrate the nuclear movements during mitosis. The progeny of the single nucleus in the center of the first image in column A are marked with a white circle. The temperature during the recording period was 23.8°C. As defined, each nuclear cycle starts with interphase and ends with the following telophase (see Foe and Alberts, 1983). (Column *A*) Metaphase of nuclear cycle 11 to interphase of nuclear cycle 12; (column *B*) metaphase of nuclear cycle 12 to interphase of nuclear cycle 13; (column *C*) metaphase of nuclear cycle 13 to interphase of nuclear cycle 14. Bar, 10 μm.

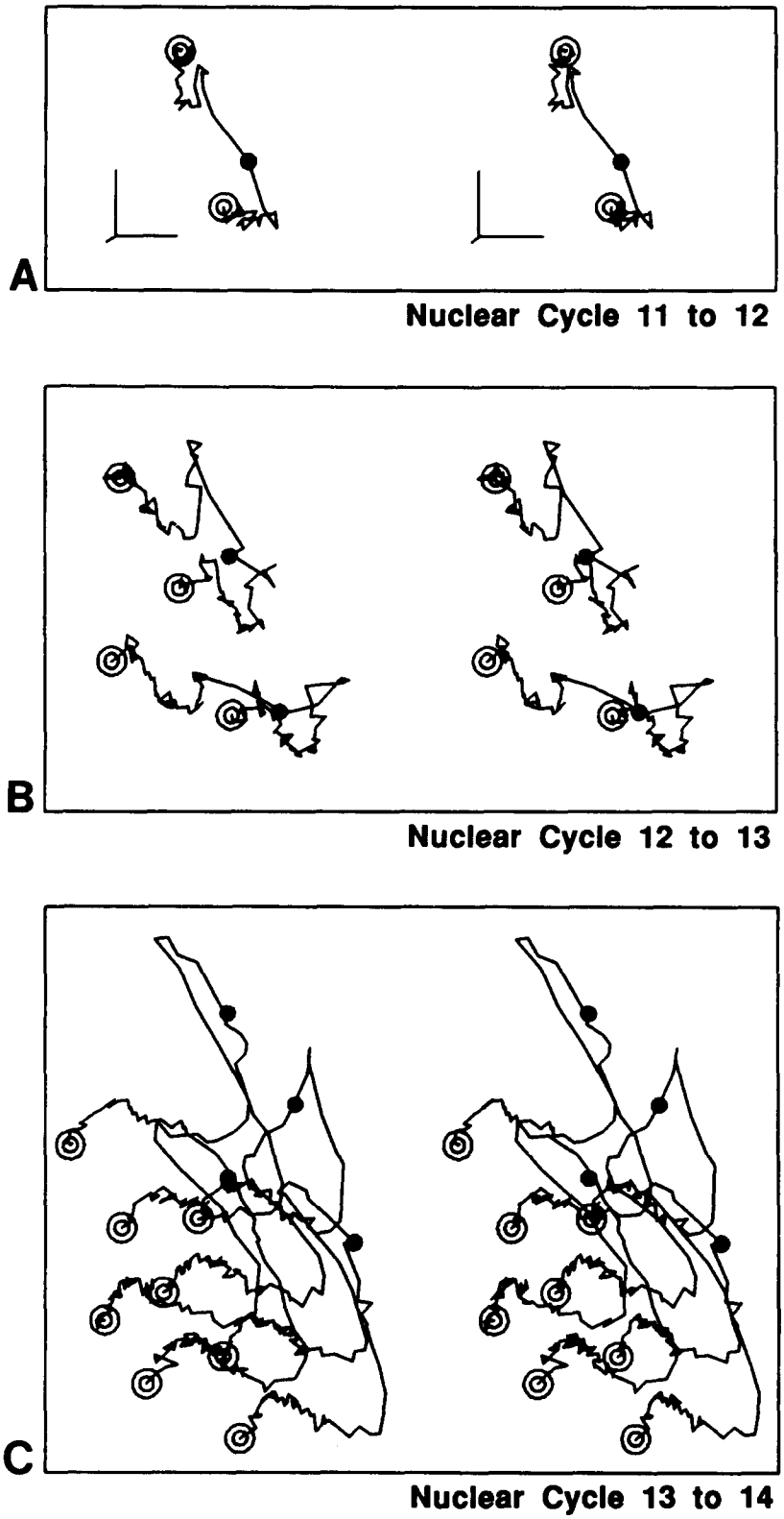

Figure 3. Computer-generated representations of tracing the movements of nuclei from metaphase of nuclear cycle 11 to interphase of nuclear cycle 14. The movements of the nuclei shown in Fig. 2 were traced at 23-s intervals and are projected here as stereo images, where each trace shows the path taken by sister nuclei as they separate from each other starting at metaphase in one cycle (*closed circles*) and continuing to metaphase in the subsequent cycle (*concentric open circles*). In this representation, the depth component increases linearly with increasing time with a straight line connecting successive positions separated by 23-s intervals. To obtain an uncluttered perspective of the nuclear movements, the models were rotated 20 degrees about both the horizontal and vertical axes (as shown by the axes in *A*). Time increases as the nuclei move away from the viewer if the stereo pairs are viewed with the aid of stereo glasses, while the opposite perspective is seen with unaided "cross-eyed" viewing. The tilt angle between left and right images is 6 degrees. (*A*) Metaphase of nuclear cycle 11 to metaphase of nuclear cycle 12; (*B*) metaphase of nuclear cycle 12 to metaphase of nuclear cycle 13; (*C*) metaphase of nuclear cycle 13 to the start of cellularization in cycle 14.

mitotic domains that are designated as domains 1, 2, 5, 6, 9, 24, and B (Fig. 1). These domain numbers have been assigned according to the temporal order of the entry of their nuclei into mitosis of cycle 14; the exception is domain B in which the cells fail to divide during the first 3 h of gastrulation (Foe, 1989). The cells within each mitotic domain also have a characteristic orientation of their mitoses; thus, the cells in domains 1, 2, 5, and 24 divide parallel to the surface of the embryo, while the cells in domain 9 divide perpendicular to this surface (Foe, 1989). To assign each cell to a par-

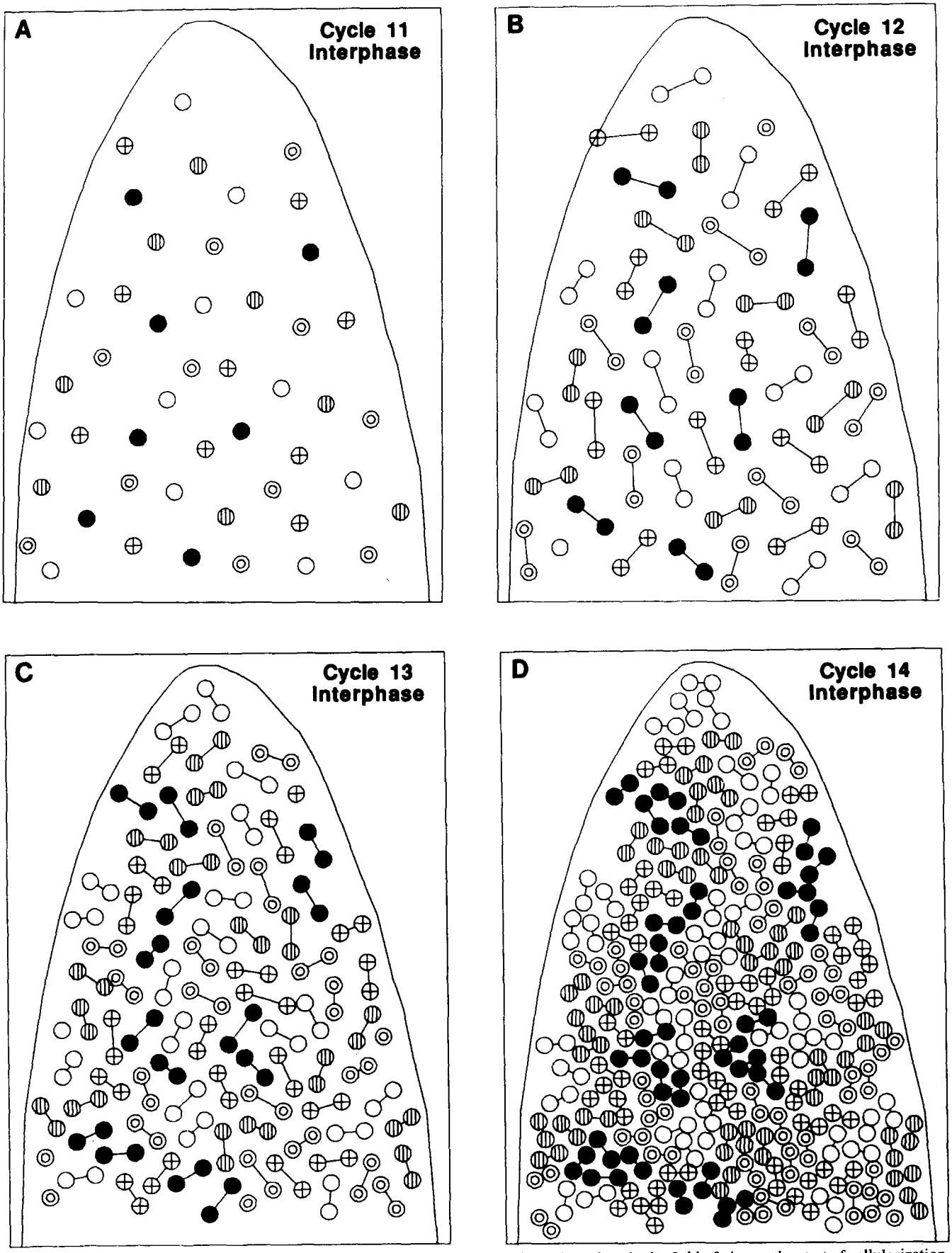

Figure 4. Map showing the lineage history of nuclei from cycle 11 to cycle 14. Each nucleus in the field of view at the start of cellularization (cycle 14 interphase) is marked with respect to its lineage history in *D*. Each lineage group is marked with a distinctive symbol starting

ticular mitotic domain, we needed to extend our recordings past the cellular blastoderm stage so as to be able to observe the time and orientation of its fourteenth division.

Tracing Nuclear Behavior after Cellularization Requires a Three-Dimensional Analysis

The task of following a cell throughout cycle 14 without losing sight of it for a short period proved to be difficult. As soon as cellularization was complete, gastrulation was initiated, and many of the cells moved out of any single focal plane. To trace the fate of all these cells simultaneously, it became necessary to view the nuclei in the living embryo in three-dimensions. This was done by recording the image from a precisely spaced series of focal planes taken at regular time intervals (Fig. 5 *A*), and computationally manipulating the data to generate a pair of stereo images. This process was repeated every 23 s to produce a time-lapse movie of the cell movements during gastrulation. A typical stereo pair of the gastrulating embryo taken from the time-lapse recording is shown in Fig. 5 *B*; the cephalic furrow can be seen in this micrograph as a horizontal line. Some of the cells in domain 1 have just completed mitosis (located in the upper-right portion of the image; also see Fig. 8 *A* for domain identification); their nuclei are smaller, more densely packed, and slightly less fluorescent. Some cells in domain 5 are in metaphase and their chromosomes are condensed to form an elongated, box-like structure (located just below and to the right of the center of the image). Because the cells that form the cephalic furrow move so deeply into the interior of the embryo, it was not possible to follow them continuously with our data set.

Cell Movements during Gastrulation

The rapid cell movements that occur during gastrulation are illustrated for three sets of lineage-related cells in Fig. 6 *A*. The unmarked end of each trace shows the starting position of a nucleus at the beginning of cellularization, while the marked end signifies either the position of the mitotic event that ends cycle 14 (circle or triangle), or the final position of a nondividing cell at the end of the recording period (square), or the last traceable position of a cell that enters the cephalic furrow (diamond). As part of a complex swirling pattern of the cell migrations, the cells first move as a mass in a posterior direction, stop for a short time, and then continue in a dorsal to ventral direction. Later in the cycle the cephalic furrow unfolds and cells at the ventral edge of the cephalic furrow begin to migrate toward the anterior pole. Together, these motions generate a clockwise vortex of cell movements.

Cells of the Same Lineage Often End Up in Different Mitotic Domains

Traces of two of the lineage-related cell groups in Fig. 6 *A* are shown as plots of cell position along the anterior–posterior axis with respect to time in Fig. 6, *B* and *C*. The nuclei move very little in the first 70 min of cycle 14. However, once cellularization is complete, the cells began to move very rapidly, traveling more than 40 μm in 15 min. The eight related cells in group 1 displayed two different fates (Fig. 6 *B*): five of the eight cells divided in the plane of the embryo surface as part of domain 1, while the other three cells of this group did not divide and could therefore be assigned to domain B. In group 2, the eight related cells had at least three different fates: two cells divided perpendicular to the surface as part of domain 9, five cells divided parallel to the surface (two as part of domain 5 and three as part of domain 24), and one cell could not be assigned because it was lost in the cephalic furrow. We conclude that clonally related cells can have very different fates with respect to mitotic domain residency.

Determining Domain Boundaries in the Gastrulation Stage Embryo

To determine the boundaries between all of the mitotic domains in the field of view, a map indicating both the orientation and the temporal sequence of the mitoses that end cycle 14 was generated (Fig. 7). In this map the orientation of division is indicated by the shape of the symbol, where circles represent cells that divide parallel to the surface of the embryo, triangles indicate cells that divide perpendicular to the surface, squares indicate cells that did not divide in the period of the recording, and diamonds indicate cells that were lost from view in the cephalic furrow. For those cells that remained visible, the time of mitosis is indicated by a clock-face; the earliest divisions are indicated by the open clock-face, while the latest divisions are indicated by the filled clock-face. The first mitotic events after cellularization occur 82 min into cycle 14 in mitotic domain 1 (for domain identification, see Fig. 8 *A*); the mitosis of cells in domain 5 begins a few minutes later and after another 11 min, the cells in domain 9 begin to divide. The cells that constitute domain 24 divide almost 50 min after the first divisions in domain 1.

Unlike the syncytial blastoderm divisions, which have irregular orientations in the surface plane, the mitoses in domains 1 and 5 are regularly oriented. In domain 1 the orientation is mostly parallel to the body axis; however, a few cells at the border with domain B divide parallel to the border, at a right angle to the body axis. The cells in domain 5 divide at a 45-degree angle to the body axis, aligned with the overall flow of the cell mass.

The variation in the temporal sequence of mitoses within a mitotic domain demonstrates that the mitotic domains do not divide synchronously, but contain temporal waves of mitoses. In domains 1 and 9 these waves appear to originate from two or more separate centers. It is not clear whether this is an indication of a finer organization of the mitotic regions.

at the end of interphase of cycle 11 (however, nuclei that share the same symbol at the start [*A*] are not related). The sister nuclei produced at the end of the preceding nuclear cycle are connected by a line for cycle 12 to 14 (*B–D*). In general, close relatives remain as neighbors and the nuclei do not mix. Occasionally, a pair of sister nuclei become separated from their six siblings by unrelated nuclei (e.g., the group with "cross-hair" symbols in the lower left portion of the map in *D*); however, this has only been seen twice in more than 10 recordings.

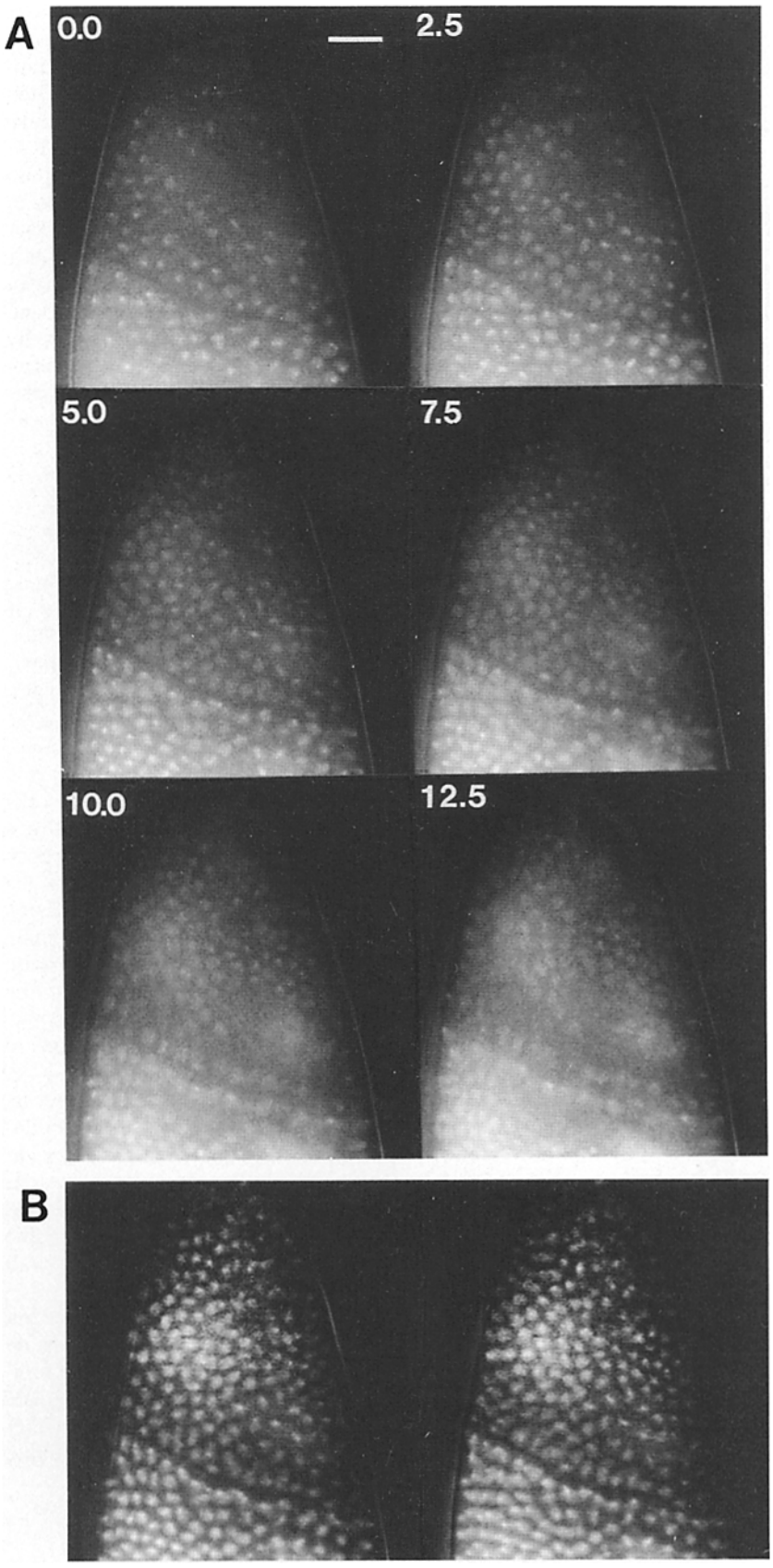

Figure 5. Obtaining three-dimensional fluorescent images of the nuclei in a gastrulation stage embryo. (*A*) Six unenhanced photographs of CCD-images taken in rapid succession, the first photograph shows the top-most focal plane; subsequent photographs proceed towards the center of the embryo at 2.5-μm intervals, as indicated by the values in the top left corner of each optical section. The time interval between the recording of each photograph (an optical section) was $\sim$3 s, this frequency is sufficient to generate three-dimensional images without blurring due to nuclear movement. The data were digitally stored and computationally enhanced and rotated in space, $\pm$15 degrees, to produce the pair of stereo images in *B*. (*B*) Stereo pair of the data set shown in *A*. The anaphase nuclei in domain 1 (for domain identification, see Fig. 8 *A*) appear less fluorescent, this is probably because of the depletion of the fluorescent-histone pool at the time of cellularization. In domain 5 several of the nuclei are in metaphase. Bar, 20 μm.

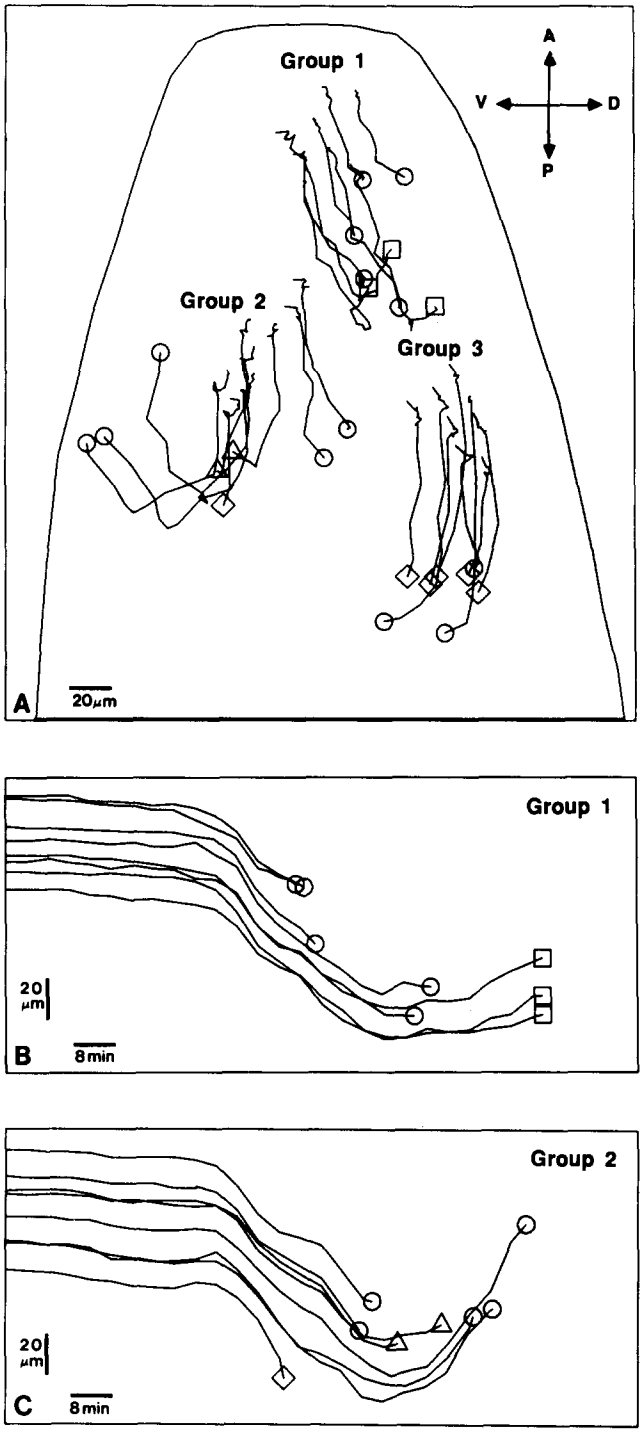

Figure 6. Computer-generated tracings of the movements of cells during cycle 14. (*A*) The movements of three lineage-related families of cells was traced from the start of cellularization (30 min into cycle 14) either until they divided or for 130 min into cycle 14. The starting end of each trace is unmarked, while the symbol at the end of each trace indicates the fate of the cell: a circle indicates that the cell divided parallel to the surface of the embryo; a triangle indicates that the cell divided perpendicular to the surface of the embryo; a square indicates that the cell did not divide; and a diamond indicates that the cell was lost from view either in the cephalic furrow or at the sides of the embryo. (*B*) Movement of the eight cells in lineage group 1 is plotted with respect to anterior–posterior position as a function of time. (*C*) Movement of the eight cells in lineage group 2 is plotted with respect to anterior-posterior position as a function of time.

Correlation of the Lineage Map with the Domain Fate Map

What might one expect to observe, using the approach described here, if the lineage of a cell was important in determining a mitotic domain? If the decision to form a particular mitotic domain is made before cycle 11, the sets of eight lineage-related cells in Fig. 4 *D* should never cross the border between two domains. If the decision to form a mitotic domain is made during interphase of cycle 11, four of the eight related cells in a group should be on one side of a domain boundary and four should be on the other side. If the decision to form a mitotic domain is instead made during cycle 12, cells should cross a domain border as pairs. Finally, if the decision to form a mitotic domain is made during cycle 13, the same pattern of single cells spanning a domain border should be observed in different embryos. On the other hand, if the decision to form a mitotic domain is entirely delayed until 14, there should be no relationship between cell lineage and mitotic domains in the embryo.

The lineage and the domain fate maps are superimposed

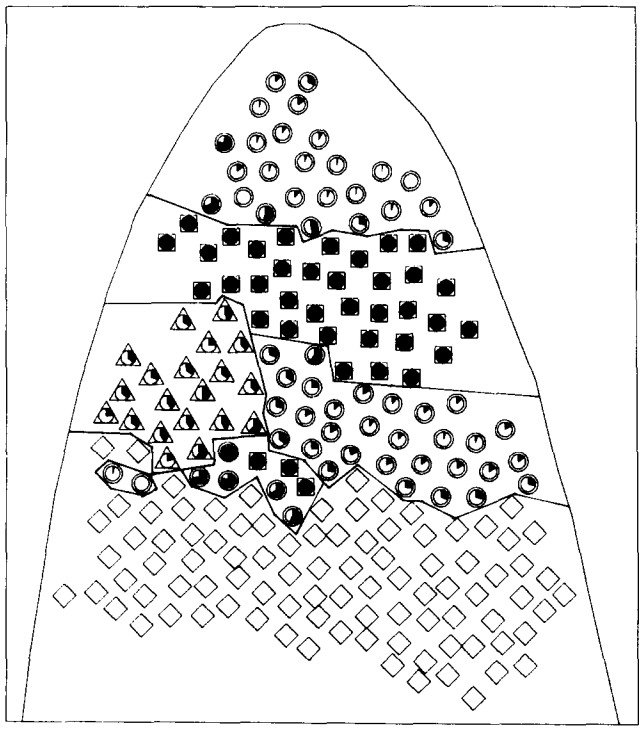

Figure 7. Identification of cycle 14 mitotic domains. This map shows the orientation of division and the division of time for the nuclei in the cycle 14 embryo, indexed on their position at the start of cellularization. Circles indicate cells that divide in the plane of the embryo, triangles indicate cells that divide perpendicular to the surface of the embryo, squares indicate cells that did not divide in the period of the recording, and diamonds indicate cells that were lost from view in the cephalic furrow. The clock-face in the center of all cells that remained visible indicates the time of division, where the open clock-face represents the earliest divisions, which occurred after 82 min of cycle 14, a half-filled clock-face represents cells that divided after 106 min of cycle 14, and the closed clock-face represents the end point of the recording 130 min after the start of cycle 14. The identifiable mitotic domains are separated by solid lines (compare with Fig. 1).

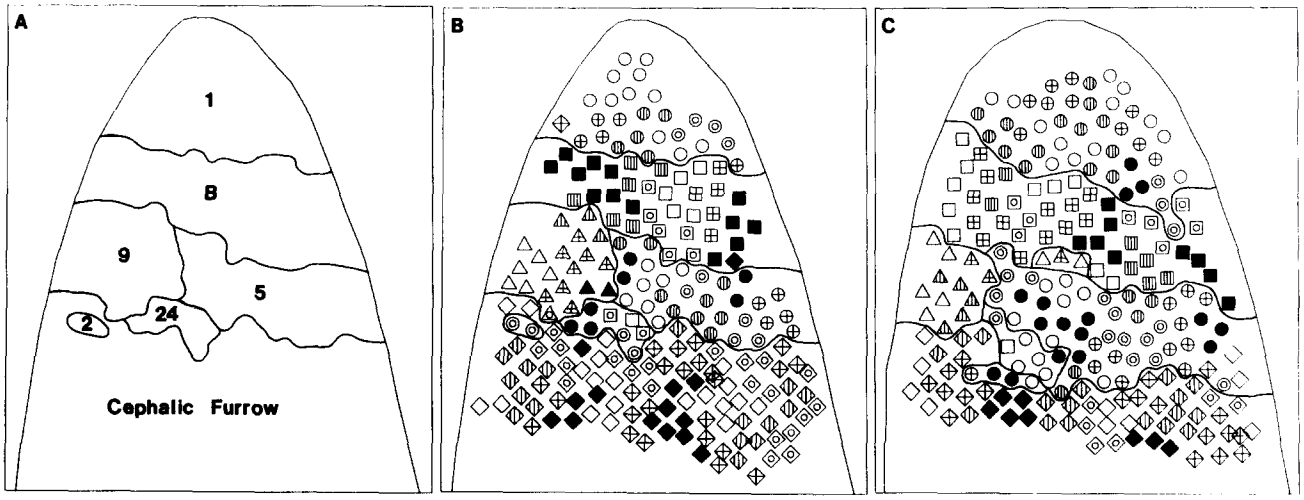

Figure 8. Fate map of the blastoderm embryo. Each cell in the cellular blastoderm stage embryo was followed from the start of cellularization until it either divided or until the end of our recording 130 min after the start of cycle 14. The fate of each cell is indicated by a different shape, where circles indicate parallel divisions, triangles indicate perpendicular divisions, squares indicate cells that did not divide, and diamonds indicate cells that were lost from view in the cephalic furrow (as in Fig. 6). The fate symbols are positioned according to the location of the nucleus at the start of cellularization. The fate symbols are also marked with respect to their lineage history according to the markings in Fig. 4 and thus represent a superposition of the lineage and fate maps. (*A*) Mitotic domains assigned according to the time and orientation of cell division. (*B*) Superposition of the lineage and the domain fate maps generated in Figs. 4 *D* and 8 *A*, respectively. This hybrid map reveals that a single lineage-related group of eight cells can have several fates. One particular group, the group with vertically striped symbols in the left-central portion of the map, had three cells in domain 9, two cells in domain 5, and two cells in domain B. (*C*) Superposition of the lineage and fate maps for a second embryo. This map confirms the results in *B*. It also demonstrates the random nature of lineage partitioning with respect to domain boundaries, since the two embryos do not correspond with respect to lineage patterns or the organization of lineages across domain borders. The only common feature is the position and shape of the mitotic domains. The differences in the size of the mitotic domains can be explained by the fact that the second embryo was rotated slightly so that the lateral midline appears shifted to the left.

in Fig. 8. The data for a single embryo (Fig. 8 *B*) show no obvious correlation between cell lineage and residency in a particular mitotic domain. For example, there are many instances of odd numbers of cells on opposite sides of a boundary between two domains and there are several cases where groups of eight cells have many different fates. These results indicate that the decision to behave one way or the other is not made until at least cycle 13.

Comparison of Lineage and Fate Maps for Two Different Embryos

If a series of lineage-dependent choices that are more complex than those described above dictate the behavior of the cells (e.g., if some decisions made earlier than others), one would expect some features of the lineage and fate maps to be maintained from embryo to embryo. A map comparing lineage and cell fate was therefore constructed for a second embryo. The results, shown in Fig. 8 *C*, show no correlation with Fig. 8 *B* in terms of the relationship between lineage and domain boundaries. The only similarity is in the overall position and shape of the mitotic patches. The lack of correspondence from embryo to embryo indicates that the domain boundaries are not drawn until cycle 14. We conclude that the decision of a cell to reside in a particular mitotic domain is probably based entirely on positional cues, with no role for cell ancestry.

Discussion

We have developed two techniques that, in combination, make it possible to follow directly the movements and divisions of individual nuclei and cells in the developing *Drosophila* embryo. The first of these is the visualization of nuclei via injection of fluorescently labeled histone proteins into syncytial stage embryos. The fluorescent histones diffuse throughout the cytoplasm and are incorporated into the chromatin, thus providing a stable, nonlethal marker for nuclear (and chromosome) structure, position, and behavior. The fluorescent histone H2A/H2B proteins are so stable in the living embryo that it is possible to visualize them in the salivary gland chromosomes of third instar larvae 4 d after the original histones were injected into embryos (data not shown). The second technique allows us to contend with the complex three-dimensional movements of the cells during gastrulation. By automatically recording a series of images at regularly spaced focal planes, three-dimensional data sets were accumulated that could be computationally transformed to generate a time-lapse, stereo-pair movie that permits the movements of a large number of cells to be traced for many hours.

Syncytial Divisions and the Lineage Map

Although the orientation of the syncytial divisions appears to be random, nuclear mixing rarely occurs. These results agree with those of Warn and Magrath (1982), who injected fluorescently labeled BSA into the space between the embryo and the vitelline membrane; during the syncytial divisions, the nuclei form protuberances in the plasma membrane that can be detected as changes in the fluorescence intensity of the labeled protein in the intervitelline space. This approach

enabled them to follow the mitotic behavior of the syncytial nuclei indirectly until gastrulation begins. In addition, Zusman and Wieschaus (1987) have demonstrated that mixing does not occur during the nuclear blastoderm divisions by showing that patches of clonally related nuclei arising from gynandomorph formation remain contiguous.

The lineage map reported here contains families of eight cells that are the descendents of a single, cycle 11 nucleus. About one quarter of the lineage-groups contain less than eight cells (12 of 47); the majority of the lineage deficits result from cells moving out of the field of view (11 of 12), while the other deficit is the result of a failed mitosis (1 of 12). This failed mitosis occurs when the chromosomes of sister nuclei fail to separate completely during anaphase, producing irregularly shaped nuclei that eventually drop out of the blastoderm monolayer into the yolkly center of the embryo. The vacancy in the monolayer is filled by the neighboring nuclei (data not shown). The syncytial embryo has an impressive capacity to repair such defects without apparently affecting normal development.

Gastrulation and the Domain Fate Map

The first movements of gastrulation occur ~70 min after the start of cycle 14 (i.e., after 70 min of interphase) and result in the formation of the cephalic and ventral furrows. The first mitotic activity begins 10 min later. The mitoses within a particular domain propagate through the domain as waves that appear to originate from multiple foci. As a mitotic wave moves away from its center, a shallow furrow forms transiently at the wave front. Cells undergoing mitosis at the advancing wave front push ahead the interphase cells that have not yet divided under the surface of the embryo. Subsequently, the cells that have just completed mitosis recoil towards the mitotic center, allowing the interphase nuclei to move back to the surface where they subsequently enter mitosis (data not shown). The significance of the multiple initiation centers in each mitotic domain and the formation of transient furrows is not yet clear; however, this sort of detailed information, which can be readily obtained from our recordings, should be important for working out the mechanics of developmental movements.

By following nuclei for >2 h from the start of cellularization, we have produced a cell-by-cell mitotic domain fate map of a small region of the embryo (Fig. 8). This fate map corresponds very well with the domain map described by Foe (1989). However, our mapping methods allow us to index the mitotic domains relative to cell position before the movements of gastrulation (e.g., at cellular blastoderm), rather than at the specific times after the start of gastrulation when the mitoses actually occur. It is interesting that the mitotic domains in the two fate maps presented in Fig. 8 appear as transverse bands approximately four cells across and that the boundary between domains 5 and 9 coincides with the lateral midline. One can speculate that this banded domain pattern is associated in some fashion with the patterned expression of the segmentation genes (for reviews see Scott and O'Farrell, 1986; Ingham, 1988).

During gastrulation, the cells in the embryo move as a continuous sheet that is never disrupted while being deformed by various invaginations and mitoses (Fig. 6). Thus, some of the regularities visible in the map of mitotic domains in Fig. 8 can easily be missed if the analysis is presented only in terms of cell positions at later times.

Effects of Cell Lineage on Cell Fate

Fate maps of the *Drosophila* embryo have previously been generated by histological examination of embryos at different developmental stages (Poulson, 1950; Hartenstein and Campos-Ortega, 1985), by analysis of gynandomorphs (Garcia-Bellido and Merriam, 1969; Janning, 1978), by an analysis of mosaic flies generated by x-ray induced mitotic recombination (Steiner, 1976; Wieschaus and Gehring, 1976; Lawrence and Morata, 1977), and by a variety of physical techniques in which small groups of cells are either transplanted, killed, or removed (Illmensee, 1976; Simcox and Sang, 1983; Lohs-Schardin et al., 1979; Underwood et al., 1980). Each of these approaches has certain limitations. Moreover, the classical fate mapping methods do not allow the experimenter to analyze the fate of individual cells directly, but are restricted to the study of more broadly defined regions of the embryo.

In spite of these caveats, the results of classical fate mapping studies have indicated that cell fate in many instances is determined at the time of cellularization, in agreement with our conclusions. It seems that the decision to reside in a particular mitotic domain is made during cycle 14 and is based on positional cues with no effect of lineage history. How these putative positional cues act is not known. However, many gene products are known to be involved in establishing the metameric compartmentation of the embryo (Gehring and Hiromi, 1986; Scott and O'Farrell, 1986; Ingham, 1988). By studying the impact of mutations affecting these genes on mitotic domain formation, we should be able to gain a better understanding of how these positional cues might be generated and maintained.

The goal of these studies was to search for a correlation between cell lineage and subsequent cell differentiation processes. In the process of addressing this question, we have developed new tools for observing the behavior of individual nuclei and cells in the living embryo in a noninvasive fashion in three dimensions. These tools are of course broadly applicable to the study of a wide variety of developmental and cellular processes on a cell-by-cell basis, and they should allow the type of detailed analysis of development that has been accomplished in *Caenorhabditis elegans* (Sulston et al., 1983) to be applied to more complex organisms.

We would like to thank Hans Chen, Yasushi Hiraoka, Andy Belmont, Michael Paddy, and Mary Rykowski for help in software development; Bill Sullivan, Kathy Miller, Doug Kellogg, Chris Field, and Bill Theurkauf for helpful discussions; and Kenneth Marians for a critical reading of the manuscript. We would especially like to thank Dr. Victoria Foe for sharing her data with us before publication.

This work was supported in part by National Institutes of Health grants GM31286-06 to B. M. Albers, GM25101-09 and GM32803-03 to J. W. Sedat, and GM31627 to D. A. Agard; and by the Howard Hughes Medical Institute (D. A. Agard and J. W. Sedat). D. A. Agard was also supported by a grant from the National Science Foundation Presidential Young Investigator Program. J. S. Minden was supported by a fellowship from the Helen Hay Whitney Foundation.

Received for publication 24 January 1989 and in revised form 17 March 1989.

References

Agard, D. A. 1984. Optical sectioning microscopy: cellular architecture in three-dimensions. *Annu. Rev. Biophys. Bioeng.* 13:191–219.

Agard, D. A., Y. Hiraoka, P. Shaw, and J. W. Sedat. 1988. Fluorescent microscopy in three dimensions. *Methods Cell Biol.* 30:353–377.

Belmont, A. S., J. W. Sedat, and D. A. Agard. 1987. A three-dimensional approach to mitotic chromosome structure: evidence for a complex hierarchical organization. *J. Cell Biol.* 105:77–92.

Foe, V. E. 1989. Mitotic domains reveal early commitment of cells in Drosophila embryo. *Development.* In press.

Foe, V. E., and B. M. Alberts. 1983. Studies of nuclear and cytoplasmic behavior in the five mitotic cycles that precede gastrulation in Drosophila embryogenesis. *J. Cell. Sci.* 61:31–70.

Foe, V. E., and G. M. Odell. 1989. Mitotic domains partition fly embryos, reflecting early cell biological consequences of determination in progress. *Am. Zool.* 29:617–652.

Garcia-Bellido, A., and J. R. Merriam. 1969. Cell lineage of imaginal discs in Drosophila gynandomorphs. *J. Exp. Zool.* 170:61–76.

Gehring, W. J. 1986. Homeotic genes and the homeobox. *Annu. Rev. Genet.* 20:147–173.

Hartenstein, V., and J. A. Campos-Ortega. 1985. Fate mapping in wild-type Drosophila melanogaster I. The spatio-temporal pattern of embryonic cell division. *Roux's Arch. Dev. Biol.* 194:181–195.

Hiraoka, Y., J. W. Sedat, and D. A. Agard. 1987. The use of a charge-coupled device for quantitative optical microscopy of biological structures. *Science (Wash. DC).* 238:36–41.

Illmensee, K. 1976. Nuclear and cytoplasmic transfer in Drosophila. *In* Insect Development. P. A. Lawrence, editor. Blackwell Scientific Publications Ltd., Oxford. 76–96.

Ingham, P. W. 1988. The molecular genetics of embryonic pattern formation in Drosophila. *Nature (Lond.).* 335:25–34.

Janning, W. 1978. Gynandomorph fate maps in Drosophila. *In* Genetic Mosaics and Cell Differentiation. W. J. Gehring, editor. Springer-Verlag, Berlin/Heidelberg. 1–28.

Lawrence, P. A., and G. Morata. 1977. The early development of mesothoracic compartments in Drosophila. An analysis of cell lineage and fate mapping and an assessment of methods. *Dev. Biol.* 56:40–51.

Lohs-Schardin, M., C. Cremer, and C, Nusslein-Volhard. 1979. A fate map for the larval epidermis of Drosophila melanogaster: localized cuticle defects following irradiation of the blastoderm with an ultraviolet microbeam. *Dev. Biol.* 73:239–255.

Palter, K. B., and B. M. Alberts. 1979. The use of DNA-cellulose for analyzing histone-DNA interactions. *J. Biol. Chem.* 254:11160–11169.

Poulson, D. F. 1950. Histogenesis, organogenesis, and differentiation in the embryo of Drosophila melanogaster meigen. *In* Biology of Drosophila. M. Demerec, editor. John Wiley & Sons, New York. 168–247.

Rabinowitz, M. 1941. Studies on the cytology and early embryology of the egg of Drosophila melanogaster. *J. Morphol.* 69:1–49.

Roberts, D. B. 1986. Drosophila: A Practical Approach. IRL Press Limited, Oxford/Washington. 38 pp.

Scott, M. P., and P. H. O'Farrell. 1986. Spatial programming of gene expression in early Drosphila embryogenesis. *Annu. Rev. Cell Biol.* 2:49–80.

Simcox, A. A., and J. H. Sang. 1983. When does determination occur in Drosophila embryos? *Dev. Biol.* 97:212–221.

Sonnenblick, B. P. 1950. The early embryology of Drosophila melanogaster. *In* Biology of Drosophila. M. Demerec, editor. John Wiley & Sons, New York. 62–176.

Steiner, E. 1976. Establishment of compartments in the developing leg imaginal discs of Drosophila melanogaster. *Wilhelm Roux's Arch. Dev. Biol.* 180: 9–30.

Sulston, J. E., E. Schierenberg, J. G. White, and J. N. Thomas. 1983. The embryonic cell lineage of the nematotode Caenorhabditis elegans. *Dev. Biol.* 100:64–119.

Turner, F. R., and A. P. Mahowald. 1976. Scanning electron microscopy of Drosophila embryogenesis I. The structure of the egg envelope and the formation of the cellular blastoderm. *Dev. Biol.* 50:95–108.

Underwood, E. M., F. R. Turner, and A. P. Mahowald. 1980. Analysis of cell movements and fate mapping during early embryogenesis in Drosophila melanogaster. *Dev. Biol.* 74:286–301.

Warn, R. M., and R. Magrath. 1982. Observations by a novel method of surface changes during the syncytial blastoderm stage of the Drosophila embryo. *Dev. Biol.* 89:540–548.

Wieschaus, E., and W. Gehring. 1976. Clonal analysis of primordial disc cells in the early embryo of Drosophila melanogaster. *Dev. Biol.* 50:249–265.

Zalokar, M., and I. Erk. 1976. Division and migration of nuclei during early embryogenesis of Drosophila melanogaster. *J. Microsc. Biol. Cell.* 25: 97–106.

Zusman, S. B., and E. Wieschaus. 1987. A cell marker system and mosaic patterns during early embryonic development in Drosophila melanogaster. *Genetics.* 115:725–736.